



Article

Night-Time Skyglow Dynamics during the COVID-19 Epidemic in Guangbutun Region of Wuhan City

Chengen Li ¹, Xi Li ^{2,*} and Changjun Zhu ¹¹ School of Remote Sensing and Information Engineering, Wuhan University, Wuhan 430079, China² State Key Laboratory of Information Engineering in Surveying, Mapping and Remote Sensing, Wuhan University, Wuhan 430079, China

* Correspondence: lixi@whu.edu.cn; Tel.: +86-180-6241-1350

Abstract: The COVID-19 epidemic lockdown has a direct influence on urban socioeconomic activity, including night-time light (NTL) changes. Night-time skyglow, a form of light pollution caused by NTL, is also affected by public emergencies. Here we investigated the impact of the lockdown on the night-time skyglow in the Guangbutun region of Wuhan, China. We monitored the night-time sky from 1 November 2019 to 12 April 2020 and compared the intraday skyglow pattern and day-to-day variation of skyglow before and during the lockdown. We found that the detected earliest shutdown timing of lights (STL) was moved from 22:00 (before the lockdown) to 21:30 (after entering the lockdown), and the fluctuation of skyglow decreased significantly during the lockdown. Furthermore, we found the night-time skyglow at various time intervals generally decreased and then recovered during the lockdown. The most severe decrease in zenith sky brightness (ZSB) was observed at the 21:30–22:00 time interval, with a decrease ratio (DR) of 72.1% and a recovery ratio (RR) of only 22.6%. On the other hand, the skyglow near midnight was the least affected by the lockdown, and the RR (32.6% and 24.3%) was comparable to the DR (30.4% and 38.2%), which means the skyglow at this time basically recovered to the pre-epidemic level. We conclude that long-term monitoring of sky brightness using single-channel photometers, such as SQMs, can provide a multi-temporal microscopic perspective for studying the dynamics of skyglow caused by human activities.

Keywords: COVID-19; lockdown; night-time light; skyglow; remote sensing; sky quality meter

**Citation:** Li, C.; Li, X.; Zhu, C.Night-Time Skyglow Dynamics during the COVID-19 Epidemic in Guangbutun Region of Wuhan City. *Remote Sens.* **2022**, *14*, 4451. <https://doi.org/10.3390/rs14184451>

Academic Editors: Martin Aubé and Andreas Jechow

Received: 27 July 2022

Accepted: 3 September 2022

Published: 6 September 2022

Publisher's Note: MDPI stays neutral with regard to jurisdictional claims in published maps and institutional affiliations.



Copyright: © 2022 by the authors. Licensee MDPI, Basel, Switzerland. This article is an open access article distributed under the terms and conditions of the Creative Commons Attribution (CC BY) license (<https://creativecommons.org/licenses/by/4.0/>).

1. Introduction

In December 2019, COVID-19 epidemic outbreak in Wuhan, China [1,2]. On 23 January, Wuhan implemented the “lockdown” policy, including shutting down sports venues, schools, tourism, and businesses [3]. According to one study conducted in Wuhan [4], there were signs of resumption of work in late March, prior to the announcement of lifting the lockdown. Wuhan’s inner-city lockdown was mainly lifted on 8 April, but some residual restrictions remained, such as postponed back-to-school dates for students. In fact, while the lockdown had successfully stopped the epidemic from spreading [5–7], it had also significantly affected people’s daily routines and social interactions, altering the natural environment and socioeconomic systems [8].

Night-time light (NTL), also known as artificial light at night (ALAN), is widely used in human activity tracking, economic dynamics analysis, disaster estimation, ecological pollution monitoring, and so on [9]. The NTL scattered back toward the earth by the atmosphere raises artificial skyglow [10]. In addition to the dynamics of the NTL sources [11–14], the night-time skyglow is also affected by atmospheric composition (such as particulate matter from air pollution [15]), meteorological events (such as clouds [16,17], moonlight [18]), and surface reflectance [19].

Night-time skyglow measurements are generally conducted on the ground, such as monitoring the temporal fluctuation of night-time sky brightness with single-channel photometers (e.g., sky quality meter, SQM) [20–22]. The approach of ground-based all-sky

night-time imaging employing calibrated consumer digital cameras with fisheye lenses is also becoming popular [23–25]. The former method is better suited for long time series observations, whereas the latter provides more spatial and spectral information, as discussed in the review of night sky brightness measurements [26].

Several studies on NTL variations in Wuhan during the COVID-19 lockdown have been conducted. Zheng et al. investigated the spatial and temporal changes of NTL and atmospheric pollutants [27], while Shao et al. and Tian et al. analyzed the work resumption of Wuhan during the late lockdown [4,28]. The majority of these research, however, focused on changes in urban illumination utilized NTL radiance data, derived from remote sensing satellites, rather than concentrating on variations of night-time skyglow or light pollution with ground-based measurements. During the COVID-19 lockdown, the observation period for research on changes in night-time skyglow with ground-based measurements is not limited to the satellite overpass time, providing previously unknown information on changes in skyglow and light pollution caused by human activities. Bustamante-Calabria et al. found there was a clear relationship between the quantity of PM10 particles and zenith sky brightness in Granada, Spain, and indicated the reduction in urban skyglow during the lockdown may be related to a reduction in urban illumination and air pollution [21]. Jechow et al. found that although there was an increase in correlated color temperature (CCT) because of the advancement of illumination technology, there was a different degree of the attenuation of skyglow in the center of and the edge of Berlin, Germany during COVID-19 lockdown [25]. They determined that the major explanation was improved air quality as a result of less traffic and air circulation.

Here, we investigated night-time skyglow dynamics for an example in Guangbutun region of Wuhan, China, under the effects of the COVID-19 lockdown. The night-time sky was continuously measured by the SQM device with high temporal resolution from November 2019 to April 2020. We retrieved the shutting timing of NTL (STL) to detect whether the intraday skyglow pattern was influenced by the lockdown. The fluctuation of the skyglow before and during the lockdown was also compared in the form of the coefficient of variation (CV). Furthermore, the decrease ratio (DR) and the recovery ratio (RR) were defined to depict the decrease and restoration of night-time skyglow during the lockdown. We have not seen other studies reporting on the dynamics of night-time skyglow in Wuhan during the COVID-19 epidemic, despite the fact that Wuhan was the first city in the world to implement the lockdown policy.

2. Materials and Methods

2.1. Study Region and Sky Quality Meter Data

Located in Wuhan, China, Guangbutun region is a typical representative of Wuhan's economic growth dynamics, and it was chosen as the target region for monitoring and analyzing night-time light pollution in this study. To the west of Guanbutun is the bustling Jiedaokou commercial district, while the north–south location is adjacent to Wuhan University and Central China Normal University, and the east side of Guangba Road is flanked by a large number of shops and residential areas. The SQM device is situated on the roof of the State Key Laboratory of Information Engineering in Surveying, Mapping, and Remote Sensing (lat = 30.528°N, long = 114.354°E, h = 40 m above mean sea level) at Wuhan University, which provides the convenience of setting up and maintaining the device due to the open campus environment. Locations and surrounding NTL sources are shown in Figure 1. Figure 1a illustrates the NTL image of Wuhan by LuoJia-1 satellite, which was launched on 2 June 2018 [29]. Because of its high spatial resolution of 130 m, LuoJia-1 can provide rich information in urban areas and has great potential for artificial light pollution investigation [30]. In addition, Figure 2 indicates the complete night-time sky and the NTL sources from the Jiedaokou commercial district, which is the major contributor to the night-time skyglow at night. Since we were unable to access the SQM observation site during the lockdown, all images in Figure 2 were taken after the lockdown was lifted, and they are only for exhibition purposes.

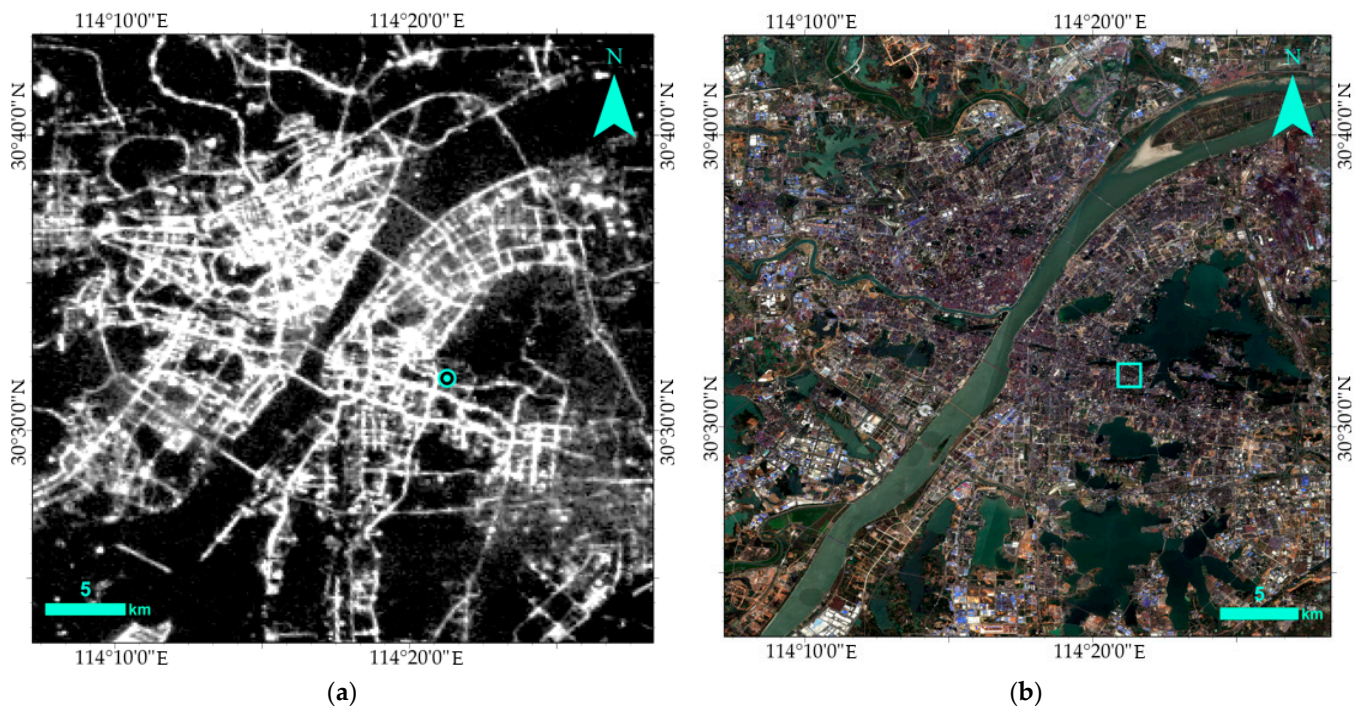


Figure 1. (a) NTL image of Luojia-1 at the study site. The dot indicates the location of the SQM device; (b) True color synthesis image of Sentinel II at the study site. Guangbutun region is framed by the square.



Figure 2. The night-time skyglow and surrounding NTL sources. (a) The image of the complete night-time skyglow induced by the moon and urban NTL with a digital camera with a fisheye lens. The red dot demonstrates the direction of the Jiedaokou commercial district; (b) The image of the Jiedaokou commercial district from the observation site; (c) The main decorative lights in the Jiedaokou commercial district.

In this study, we chose the SQM-LU-DL model, which mainly measures the average brightness of the zenithal region with a full width half maximum (FWHM) view angle of 20° . The SQM documents the night-time sky brightness in the form of magnitudes per square arcsecond ($\text{mags}/\text{arcsec}^2$) with a precision of 10%, i.e., $0.1 \text{ mags}/\text{arcsec}^2$. It should be noted that the SQM logarithmically measures night-time sky brightness in astronomical units. The recorded value of SQM decreases as the skyglow increases, which is counter-intuitive to non-astronomers. Previous research has shown long-term stability of SQM measurements with a minimal annual variation [31], which is appropriate for our study. After a few days of adjustment and calibration, on 1 November 2019, we began to monitor

the night-time sky with a high temporal frequency of two minutes. We continuously collected astronomical brightness data in mags/arcsec² until the dawn of 12 April 2020. Winter lasts from December to February in Wuhan, and the weather warms up in March and early spring, with an overall temperature difference of less than 10 °C between spring and winter. As the SQM devices have been tested stable and adequate for use in the environment over the range of −15 °C to 35 °C [32], it can be assumed that seasonal factors, such as temperature, had a limited impact on the dynamics of night-time skyglow in this period. Belonging to humid subtropical monsoon climate, Wuhan has a high frequency of rainfall despite abundant sunshine in both winter and spring (as shown in Table 1), which makes many of our observation records invalid. Therefore, we must preprocess the obtained SQM records time series and remove invalid records. Using the operation software provided by Unihedron (available online: <http://unihedron.com/projects/darksky/cd/>, accessed on 7 July 2021), we exported the time series of the astronomical sky brightness before and during the entire lockdown of the device.

Table 1. Meteorological data for Wuhan City by month from November 2019 to April 2020. Data obtained from Wuhan Statistical Yearbook 2020 and 2021 (available online: <http://tjj.wuhan.gov.cn/tjfw/tjnj/>, accessed on 21 June 2022).

Month	Average Temperature (°C)	Sunshine Hours (h)	Number of Rainy Days (day)	Volume of Precipitation (mm)
November	12.9	108.3	10	56.7
December	6.5	103.5	7	27.1
January	4.1	93.9	16	113.2
February	8.6	173.4	10	106.9
March	13.0	224.7	12	84.4
April	16.8	212.5	7	45.9

2.2. Preprocessing of Data

2.2.1. Removal of Cloud-Influenced Data (Including Snow and Ice Reflections)

In the study on the function of urban clouds in the night-time light environment [33], the urban light pollution observation results were found to be influenced by cloud height, optical thickness, single scatter albedo, and asymmetry parameter. In order to reduce the effect of natural factors, such as clouds on SQM records series, the SQM records during the cloud cover (including snow and ice reflections) period must be removed. In this study, we used the NASA's Black Marble night-time lights product suite (VNP46) jointly with the fluctuation threshold of SQM records series to remove the data impacted by clouds, etc.

NASA's daily Black Marble night-time lights product suite (VNP46A1), with a 500 m spatial resolution, has been accessible at NASA's Atmosphere Archive & Distribution System (LAADS) Distributed Active Archive Center (DAAC) since January 2012 [34]. The daily data can be employed for dynamic analysis of short-term events, such as public emergencies [35,36]. The QF_Cloud_Mask Science Data Set (SDS) in VNP46A1 is used to record the cloud mark flag and snow/ice flag of the target area at the corresponding moment of data recording. The VNP46 product was generated from data from the Visible Infrared Imaging Radiometer Suite (VIIRS) Day/Night Band (DNB) onboard the Suomi National Polar-orbiting Platform (SNPP), with an overpass time of 1:30 am local time. Therefore, we can confirm the weather conditions at the observation site at the exact time of night (<https://ladsweb.modaps.eosdis.nasa.gov/>, accessed on 24 August 2021). In this study, the cloud mask flag in VNP46A1 was used to determine the sure cloud influence time period, and the snow/ice flag was used to determine the period impacted by snow and ice cover.

Furthermore, the determination of whether the skyglow was affected by clouds throughout the night depends not only on weather information at certain moments but also on the fluctuation of the SQM records series. Cloudless periods were chosen based on the criterion of no flickering in SQM readings with a standard deviation less than

0.1 mags/arcsec² [21]. Here, we found that the standard deviation of the filtered half-hour SQM data series was controlled within 0.1 mags/arcsec² when the variation threshold was set to 0.1 mags/arcsec² before midnight and 0.05 mags/arcsec² after midnight. As a result, we obtained smoothly fluctuating series before and during the lockdown. The monotone increasing or decreasing series between the two smoothly fluctuating series were also kept because they are more likely to be caused by human activities, such as turning on or off lights.

2.2.2. Removal of Moon-Influenced Data

SQM readings are particularly sensitive to the moon phase and moon elevation. Although this sensitivity decreases in developed urban regions, it cannot be ignored. The overall effect of the moon burst on the urban skyglow is small in areas with a high amount of artificial illumination, but it still causes the night-time sky brightness to vary periodically with the moon phase [18]. We generated the moon phase and moon elevation series for the SQM records series by using the “.dat to Moon csv” tool of operation software Unihedron Device Manager (1.0.0.318) provided by Unihedron (available online: <http://unihedron.com/projects/darksky/cd/>, accessed on 7 July 2021). To entirely remove the influence of the moon on the time series of sky brightness, we only analyzed data with moon elevation angles below 0°. The moon-impacted SQM records series were just displayed to ensure data consistency and were not used in quantitative analysis. Figure 3 takes the night from 18 to 19 November 2019 as an example to indicate the detailed process of the removal of data under the effect of moonlight. As the moon rose over the horizon at 22:34 this night, the SQM records after 22:34 were removed.

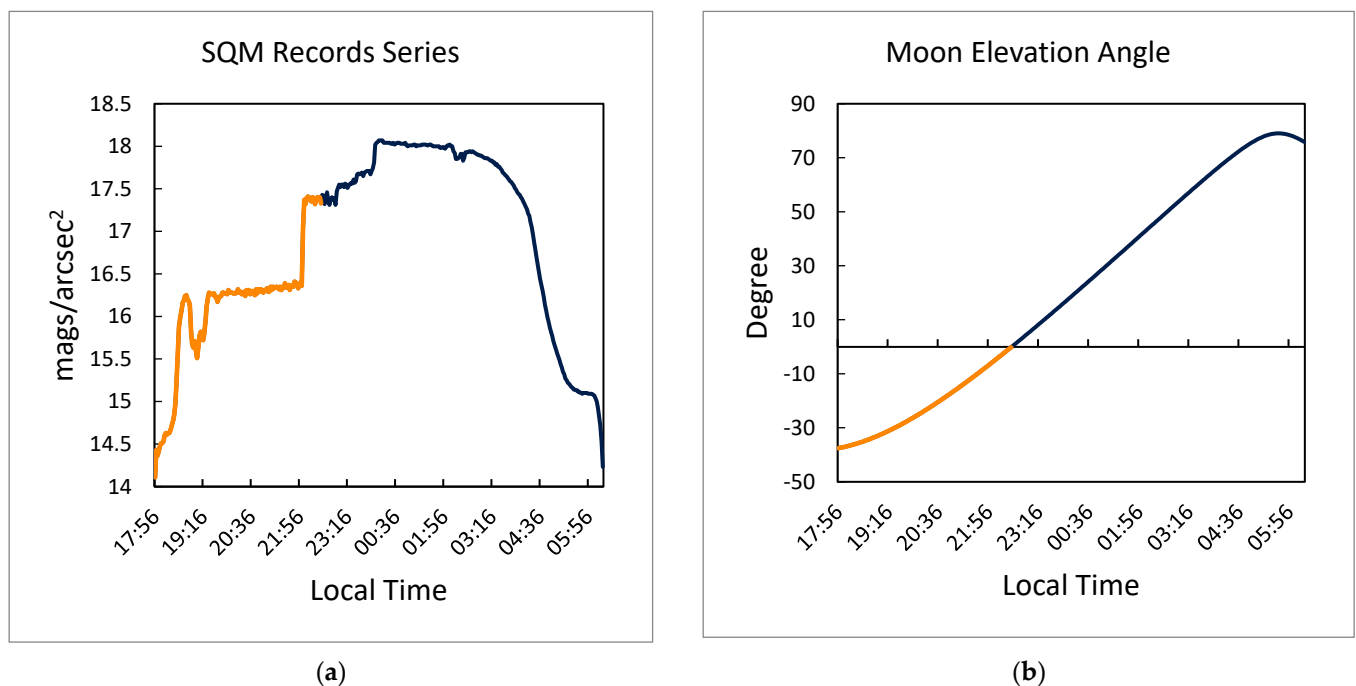


Figure 3. (a): The SQM records series obtained between 17:56 18 November and 6:20 November 2019; (b): The generated moon elevation angle (-90° – 90°) series for the SQM records series. Only the SQM records acquired before 22:34 were retained (the orange part) to remove the impact of the moon.

2.3. Methods

2.3.1. Shutdown Timing of Lights (STL)

The NTL sources of Guangbutun region consist mainly of permanent illumination (such as street lights) as well as decorative lights (such as electronic billboards), forming intraday skyglow patterns in this area. The decorative lights are gradually turned off near midnight, when the SQM measurements show an abrupt rise with the decline of

skyglow. Here, we defined the shutdown timing of lights (STL) to describe the moment when the detection of a light closure has occurred. We generated the differential sequences of the SQM records and exerted all the STLs from the SQM differential sequences. A lighting closure is determined to happen when the difference between two consecutive SQM readings is larger than 0.1 mag/arcsec^2 . The form is as in Equation (1):

$$\text{STL} = T_{i+1}, m_{i+1} - m_i > 0.1 \quad (1)$$

where T_i and T_{i+1} denote the i th and $(i + 1)$ th SQM observation moment; m_i and m_{i+1} denote the i th and $(i + 1)$ th SQM readings.

In this work, we compared the STLs before and during the lockdown to figure out how these decorative lighting functions changed as a result of the COVID-19 lockdown.

2.3.2. Coefficient of Variation (CV)

Traffic-induced lights and some decorative lights are dynamic, making the night-time sky brightness fluctuate up and down over time. As these flickering light sources constitute a key component of urban NTL, it is critical to investigate the fluctuation of night-time skyglow before and during the epidemic. Here, we defined the coefficient of variation (CV) of the SQM records series to describe the fluctuation of night-time skyglow at different time intervals (Equation (2)):

$$\text{CV} = \frac{\sigma}{\bar{m}} \quad (2)$$

where σ is the standard deviation of the SQM records series; \bar{m} is the average of the SQM records series.

2.3.3. Decrease Ratio (DR) and Recovery Ratio (RR)

Considering that the mags/arcsec^2 is logarithmic and counter-intuitive, it is not suitable to be used directly to depict the intensity of the night-time skyglow. According to the user manual, mags/arcsec^2 can be converted by the formula as in Equation (3) to the luminance unit cd/m^2 [37]. Here, we transformed the daily mean of the SQM records at various time intervals into zenithal sky brightness (ZSB) by Equation (3) to represent the intensity of the night-time skyglow and calculate the DR at different time intervals. The form is as in Equation (3):

$$\text{ZSB} = 10.8 \times 10^4 \times 10^{-0.4 \times \bar{m}} \quad (3)$$

where ZSB is the zenith brightness of the night-time sky; \bar{m} is the average of SQM readings at a specific time interval.

We found there was a general decrease and recovery of night-time skyglow at various time intervals during the COVID-19 epidemic lockdown, as shown in Section 3.3. We defined the decrease ratio (DR) of the skyglow to quantitatively depict the reduction degree of the skyglow at different time intervals after entering the lockdown as Equation (4):

$$\text{DR} = \frac{\text{ZSB}_P - \text{ZSB}_D}{\text{ZSB}_P} \quad (4)$$

where ZSB_D and ZSB_P are the average zenithal sky brightness during the dark period and prior to the lockdown.

The dark period of the skyglow is determined based on the day-to-day trend of the SQM records series, as shown in Section 3.3. Similarly, we determined the recovery period and defined the recovery ratio (RR) to quantitatively measure the recovery effect of night-time skyglow at different time intervals (Equation (5)).

$$\text{RR} = \frac{\text{ZSB}_R - \text{ZSB}_D}{\text{ZSB}_P} \quad (5)$$

where ZSB_R , ZSB_D , and ZSB_P are the average zenithal sky brightness during the recovery period, the dark period, and prior to the lockdown.

3. Results

3.1. Effect of Lockdown on the Intraday Skyglow Pattern

Figure 4 shows a comparison of astronomic sky brightness in Guangbutun region of Wuhan, China, on clear and moonless nights prior to lockdown and during lockdown. The sky brightness series did not change much after midnight from 1 November 2019 to 12 April 2020. In addition, before midnight, sky brightness in Guangbutun region caused by NTL exhibited the following features:

1. The urban sky darkened in stages over time;
2. The sky brightness varied quickly, generally within a few minutes, and most of the time it was fluctuant;
3. Changes in sky brightness were mainly at full or half clock.

Night-time Astronomical Sky Brightness (Guangbutun Region)

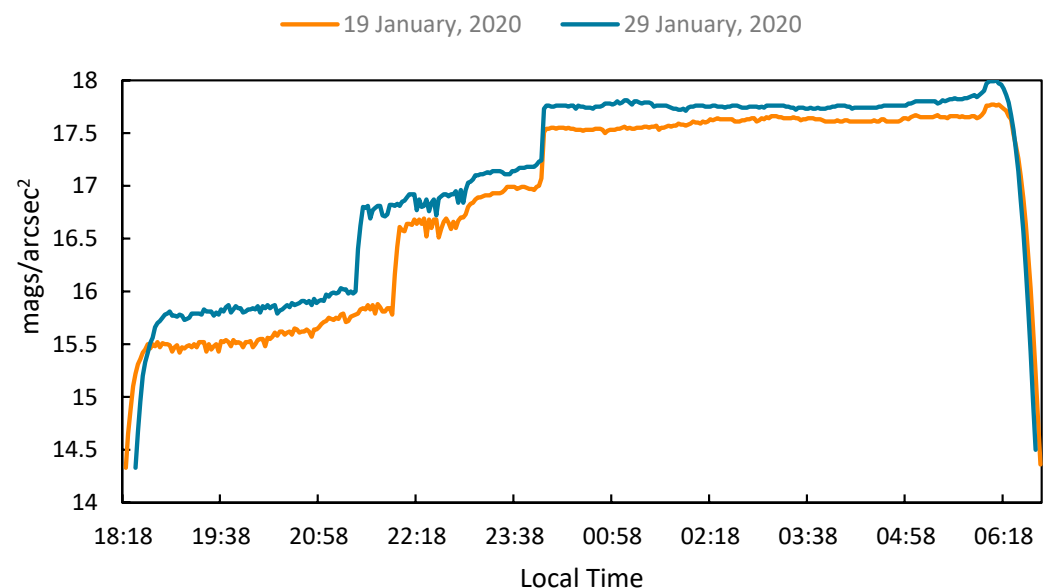


Figure 4. The night-time sky brightness series of Guangbutun region obtained with the SQM device. Note that 19 January 2020 is prior to the COVID-19 lockdown and 29 January 2020 is during the lockdown.

After entering the lockdown, this intraday skyglow pattern was largely maintained, but we perceived some changes. We extracted all the shutdown timings of lights (STLs) on clear and moonless nights during the SQM monitoring period. Figure 5 shows the variation of the earliest detected STLs on different nights prior to lockdown and during lockdown. Before the COVID-19 epidemic, the earliest STL was focused around 22:00. Nevertheless, the observed earliest STL was advanced after entering the lockdown. Beginning with 28 January 2020, the earliest STL was pushed forward from 22:00 to 21:30; following 17 February, the earliest STL was pushed forward to 21:00 again. It was not until 17 March that the earliest STL started to recover. Even after lifting the lockdown, the earliest STL of 11 April was at 21:30, indicating that the part of lighting did not entirely return to the pre-lockdown state.

The Daily Trend of the detected earliest STL

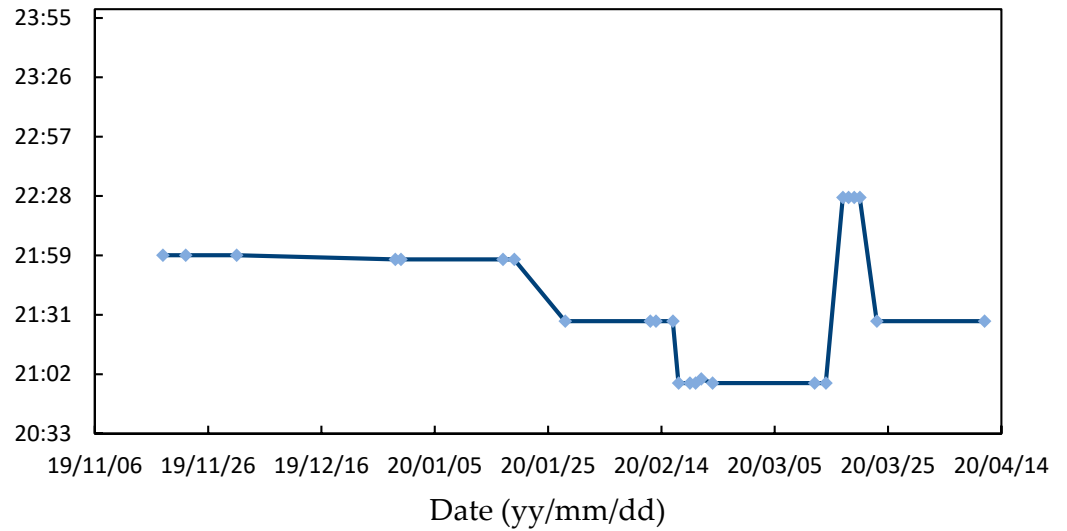


Figure 5. The earliest detected STLs from 1 November 2019 to 12 April 2020.

We found that the intraday night-time skyglow pattern after midnight was mostly produced by permanent base illumination, which was less impacted by the lockdown. On the other hand, non-permanent artificial light sources, such as decorative lights, were the main contributors to the skyglow pattern before midnight, which were more affected by the lockdown, primarily in the form of prior closing times.

3.2. Effect of Lockdown on the Fluctuation of Skyglow

We calculated the coefficients of variation (CV) of the daily SQM record series at different times of night and divided them into two groups. The first group relates to the fluctuation of pre-lockdown skyglow, whereas the second corresponds to the fluctuation of lockdown skyglow. Considering the intraday skyglow pattern, we chose four typical time intervals: 20:30–21:00, 21:30–22:00, 23:30–24:00, and 0:00–1:00. Figure 6 shows the average CV in the four representative time intervals prior to lockdown and during the lockdown.

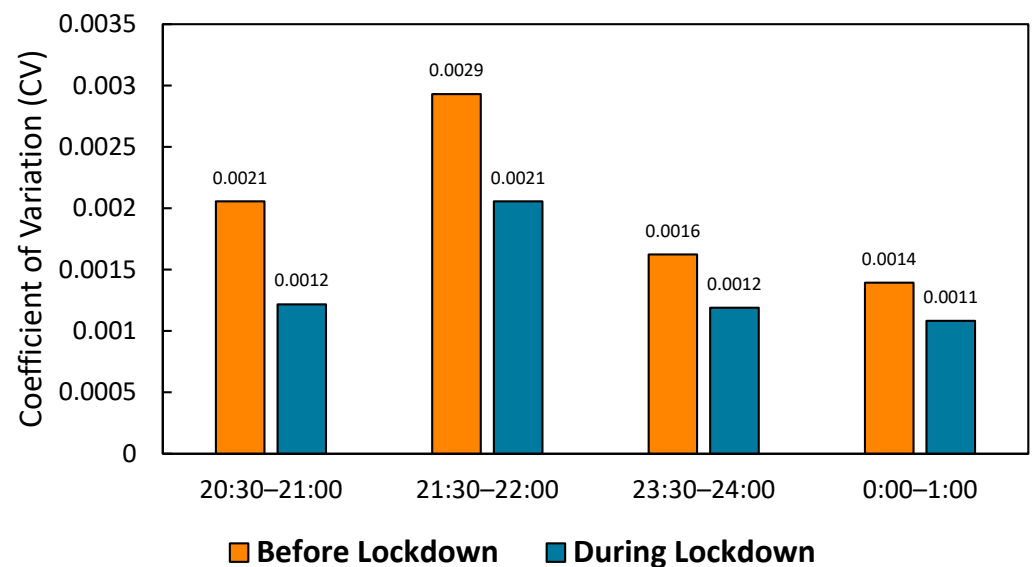


Figure 6. Average coefficients of variation (CV) at four typical time intervals before and during the COVID-19 lockdown.

The largest CV of the SQM records series happened at the 21:30–22:00 time interval; the lowest was around midnight; and the CV at the 20:30–21:00 time interval was in the middle. After entering the lockdown, the CV of the SQM records series at the four time intervals also exhibited the same characteristics. During the COVID-19 lockdown, the fluctuation of all time intervals dropped significantly, since urban traffic and residential activities were greatly limited. Moreover, the lockdown has a greater impact on the 20:30–21:00 and 21:30–22:00 time intervals, when the CV decreases by 0.0009 and 0.0008, respectively. This indicates that there was a more significant decline in the flickering light sources before midnight than after midnight during the lockdown.

3.3. Effect of Lockdown on the Day-to-Day Skyglow Dynamics

Due to the intraday skyglow pattern, we divided the sky brightness series during clear and cloudless hours before midnight (20:00–24:00) into half-hour intervals. Because the sky brightness in Guangbutun region remained steady after midnight, the latter half of the night (0:00–4:00) was presented as a distinct time interval. Figure 7 depicts the daily astronomical average sky brightness trends for four typical time intervals, 20:30–21:00, 21:30–22:00, 23:30–24:00, and 0:00–4:00, from 1 November 2019 to 12 April 2020, in reference to the duration of the cloudless and moonless sky brightness series for each time period (Table 2).

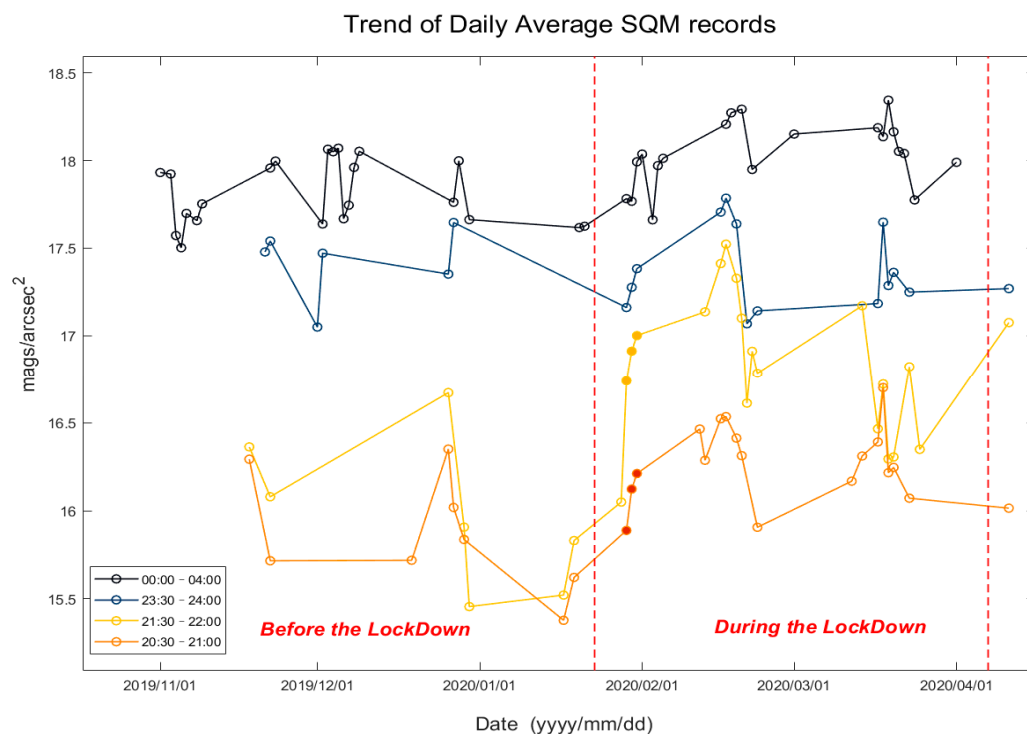


Figure 7. From 1 November 2019 to 12 April 2020, the trend of daily mean SQM measurements at various time intervals. Some of the data influenced by the moon is displayed here and solidly marked, which was not used in further quantitative analysis.

The skyglow in Guangbutun region of Wuhan, China, went through four stages:

- 1 November 2019 to 19 January 2020: Guangbutun region had not yet entered the lockdown, and the night-time urban sky was quite bright;
- 28 January 2020 to 31 January 2020: During the four days of the lockdown, there was a significant rise in SQM measurements, indicating a quick reduction in sky brightness. Note that this trend went against the increasing brightening effects of the moon. The moon was getting close to full and the moon elevation was rising these days;
- 12 February 2020 to 20 February 2020 (The Dark Period): The night-time sky brightness stopped falling and stabilized, reaching its lowest point at 17 February 2020;

- 21 February 2020 to 12 April 2020 (The Recovery Period): The night-time sky brightness increased dramatically on 21 February, and the recovery stage began.

Table 2. Number of days of cloudless and moonless SQM records series from 1 November 2019 to 12 April 2020. Due to cloud and moon interference, the length and members of the dates vary during different time intervals.

Time Interval	Number of Days
20:00–20:30	23
20:30–21:00	23
21:00–21:30	23
21:30–22:00	24
22:00–22:30	24
22:30–23:00	21
23:00–23:30	18
23:30–24:00	20
24:00–04:00	42

We noticed that the night-time urban skyglow at different time intervals decreased after entering the lockdown. From 12 February 2020, the night-time sky brightness stopped dropping rapidly and started to rebound from 21 February. Therefore, we determined the period from 12 February to 20 February as the dark period and set the period from 21 February to 12 April as the recovery period. We transformed daily averaged SQM records into zenithal sky brightness (ZSB) to measure the decline and resumption effects during the dark period and recovery period, and the specific daily ZSB values at different intervals are recorded in Table 3. As shown in Figure 8, we compared the average ZSB of various time intervals at different stages. Meanwhile, we quantitatively calculated the decrease ratio (DR) and recovery ratio (RR) of night-time skyglow at each time interval, as shown in Table 4.

Table 3. The daily ZSB values at all time intervals from 1 November 2019 to 11 April 2020. Note that the dates of ZSB values after midnight are advanced by one day to maintain temporal consistency, which means the ZSB value at the 0:00–4:00 time interval of 1 November in Table 3 was recorded at the dawn of 2 November.

Date	Zenithal Sky Brightness (mcd/m ²)								
	20:00–20:30	20:30–21:00	21:00–21:30	21:30–22:00	22:00–22:30	22:30–23:00	23:00–23:30	23:30–0:00	0:00–4:00
1 November 2019	/	/	47.4	/	/	/	/	/	7.3
2 November 2019	/	/	/	/	/	/	/	/	7.3
3 November 2019	/	/	/	/	/	/	/	/	10.1
4 November 2019	/	/	/	/	/	/	/	/	10.8
5 November 2019	/	/	/	/	/	/	/	/	9.0
7 November 2019	/	/	/	/	/	/	/	/	9.3
8 November 2019	/	/	/	/	/	/	/	/	8.6
18 November 2019	33.2	32.8	31.8	30.8	12.1	/	10.3	/	/
20 November 2019	37.6	/	/	/	/	/	/	/	/
21 November 2019	/	/	/	/	/	/	/	11.0	7.1
22 November 2019	56.9	55.9	42.7	40.0	15.5	14.7	11.4	10.4	6.8
1 December 2019	/	/	/	/	19.6	/	18.6	16.3	9.5
2 December 2019	/	/	/	/	/	15.3	12.4	11.1	6.4
3 December 2019	/	/	/	/	/	/	/	/	6.5
4 December 2019	/	/	/	/	/	/	/	/	6.4
5 December 2019	/	/	/	/	/	/	/	/	9.3
6 December 2019	/	/	/	/	/	/	/	/	8.6
7 December 2019	/	/	/	/	/	/	/	/	7.1
8 December 2019	/	/	/	/	/	/	/	/	6.5
19 December 2019	50.2	55.7	62.8	/	/	/	/	/	/
26 December 2019	31.1	31.1	26.8	23.2	/	/	13.8	12.4	8.5
27 December 2019	42.4	42.3	/	/	/	/	/	9.4	6.8
29 December 2019	/	50.0	/	46.8	20.0	/	/	/	9.3
30 December 2019	/	/	/	71.0	/	/	/	/	/
17 January 2020	/	76.2	67.8	66.8	24.7	26.8	/	/	/
19 January 2020	65.1	60.9	54.3	50.3	24.1	23.7	/	/	9.7
20 January 2020	/	/	/	/	/	25.2	/	/	9.6

Table 3. Cont.

Date	Zenithal Sky Brightness (mcd/m ²)								
	20:00–20:30	20:30–21:00	21:00–21:30	21:30–22:00	22:00–22:30	22:30–23:00	23:00–23:30	23:30–00:00	0:00–4:00
28 January 2020	/	/	/	41.1	37.0	26.9	/	/	8.3
29 January 2020	/	/	/	/	19.6	19.0	15.5	14.8	8.4
30 January 2020	/	/	/	/	/	15.7	13.3	13.3	6.9
31 January 2020	/	/	/	/	/	/	12.0	12.0	6.6
2 February 2020	/	/	/	/	/	/	/	/	9.3
3 February 2020	/	/	/	/	/	/	/	/	7.0
4 February 2020	/	/	/	/	/	/	/	/	6.7
12 February 2020	26.9	28.0	26.2	/	/	/	/	/	/
13 February 2020	32.7	33.0	32.1	15.1	/	/	/	/	/
16 February 2020	27.4	26.6	24.9	11.7	10.4	10.3	8.9	8.9	5.6
17 February 2020	28.3	26.2	14.9	10.6	9.5	9.4	8.3	8.3	5.3
19 February 2020	29.7	29.4	16.0	12.6	11.4	11.2	9.7	9.5	5.2
20 February 2020	32.6	32.2	17.8	15.6	/	14.0	/	/	/
21 February 2020	50.8	/	31.4	24.5	20.8	19.7	16.8	16.1	7.1
22 February 2020	/	/	/	18.6	16.9	/	/	/	/
23 February 2020	46.4	46.9	25.9	20.9	17.6	17.9	/	15.0	/
29 February 2020	/	/	/	/	/	/	/	/	5.9
12 March 2020	36.8	36.8	21.9	/	/	/	/	/	/
13 March 2020	/	/	27.2	/	19.4	/	/	/	/
14 March 2020	32.7	32.3	17.9	14.6	13.2	12.5	11.8	/	/
16 March 2020	/	/	/	/	/	/	/	/	5.7
17 March 2020	34.3	30.0	29.1	28.0	27.8	14.2	14.0	14.4	6.0
18 March 2020	22.5	22.6	22.2	22.1	21.4	9.4	9.3	9.4	5.0
19 March 2020	35.1	35.2	33.7	32.8	31.8	14.0	13.5	13.1	5.9
20 March 2020	34.2	34.3	33.0	32.5	29.7	12.7	12.1	12.3	6.5
21 March 2020	/	/	/	/	/	/	/	/	6.6
23 March 2020	42.8	40.3	38.2	20.2	18.0	14.3	13.7	13.6	8.4
24 March 2020	/	/	/	/	15.9	/	/	/	/
25 March 2020	/	/	/	31.2	/	/	/	/	/
31 March 2020	/	/	/	/	/	/	/	/	6.9
11 April 2020	42.1	42.4	/	16.0	13.8	/	/	/	/

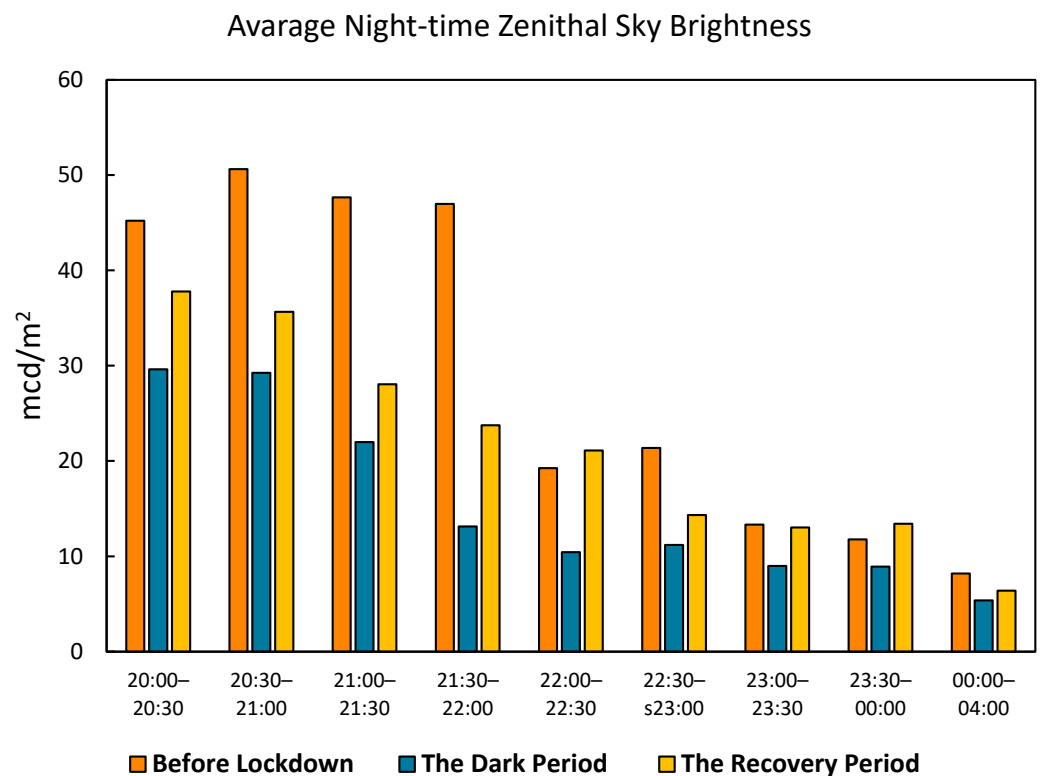


Figure 8. The average zenithal sky brightness (ZSB) at various time intervals during the three periods.

Table 4. The decrease ratio (DR) and recovery ratio (RR) of night-time skyglow at each time interval during the COVID-19 lockdown.

Time Interval	Decrease Ratio (DR)	Recovery Ratio (RR)
20:00–20:30	34.5%	18.1%
20:30–21:00	42.2%	12.6%
21:00–21:30	53.9%	12.7%
21:30–22:00	72.1%	22.6%
22:00–22:30	45.8%	55.5% *
22:30–23:00	47.6%	14.7%
23:00–23:30	32.6%	30.4%
23:30–24:00	24.3%	38.2%
24:00–04:00	34.4%	12.4%

* The RR at the 22:00–22:30 time interval was overestimated because the earliest STL was pushed forward to 22:30 from 17 March to 20 March, increasing the average ZSB. However, this phenomenon lasted just four days, and the earliest STL was pushed forward again to 21:30 beginning on 23 March. Therefore, we did not analyze the recovery effect at the 22:00–22:30 time interval.

There was a general decrease in average ZSB after entering the lockdown, and the sensitivity of urban night-time skyglow to the lockdown policy varied over time. The average ZSB dropped by 15.6 mcd/m² and 21.4 mcd/m² from 20:00 to 21:00 during the dark period, meaning DRs of 34.5% and 42.2%, respectively. As the clock approached midnight, the average ZSB only decreased by 3–5 mcd/m² due to the already gloomy night-time sky, although the DRs of these time intervals are over 20%. However, there was an alarming decline in average ZSB during 21:00 and 23:00 (25.7, 33.8, 8.82, and 10.18 mcd/m², respectively), implying that the skyglow was reduced by about half. Among these time intervals, the most negative effect of the lockdown occurred at the 21:30–22:00 time interval, when the average ZSB was reduced by 72.1%.

Furthermore, the recovery of night-time urban skyglow also varied at different time intervals during the recovery period. The best recovery was near midnight, when the RRs exceeded 30%. For example, the average ZSB between 23:30–24:00 entirely recovered later in the lockdown (13.4 mcd/m², compared to 11.8 mcd/m² before the lockdown). During the hours of 23:00–23:30, the average ZSB also basically rebounded to the pre-lockdown level (13.0 mcd/m², compared to 13.3 mcd/m² prior to the lockdown). The recovery of sky brightness was somewhat poorer after midnight, reaching only 78% of the original level (RR = 12.4%), as was the case from 20:00–21:00, reaching 84% and 70% (RR = 18.1% and 12.6%), respectively. The worst recovery period also occurred at the 21:30–22:00 time interval, with a rebound to only 51% of the previous level (23.7 mcd/m², compared to 44.0 mcd/m² before the lockdown). However, we perceived its potential for rapid restoration because the RR at the 21:30–22:00 time interval was over 20%.

4. Discussion

4.1. Variability of Night-Time Skyglow Reduction and Recovery at Different Time Intervals

At the start of the night, coupled with business activities, decorative lights in commercial districts dominate the urban night-time skyglow in Guangbutun region. These lights were partially closed upon entering the lockdown and began to reopen in the later stages of the lockdown because of the positive situation of the epidemic and work resumption, but it was difficult to return to pre-epidemic levels in the short term with RRs less than 20%. As a result, the change in skyglow during the lockdown at these times may be a reflection of the impact of the epidemic on urban total NTL.

The night-time skyglow from 21:00 to 23:00 was not stable and varied greatly from day to day before the lockdown. Furthermore, the decline in skyglow was compounded as the lockdown forced part of urban illumination to turn off earlier at these time intervals. The lighting shutdown timing was not altered to the same as before the epidemic when the lockdown was lifted, thus the recovery of the sky brightness at this time was still confined by the lighting pattern and was the least effective. As a result, we suggest

that 21:00–23:00 periods may be the most sensitive time of night-time skyglow to human activities, vulnerable to the impact of public emergencies, and that changes in NTL and light pollution should be monitored during this period.

Around midnight, lighting directly associated with commercial activity in Guangbutun region was generally switched off, and permanent urban illumination was a major contributor to the night-time skyglow. However, the recovery of sky brightness after midnight did not go as planned, with a recovery ratio of only 12.7%. The constraining reason should be the improved air quality caused by the lockdown. The early radiative transfer models have indicated that the sky brightness perceived close to the city center rises with urban aerosol concentration [38]. The recent study on skyglow during COVID-19 epidemics also mentioned a correlation between observed SQM readings and air pollution parameters, such as PM10, with more severe air pollution often being associated with a brighter night sky [21]. In fact, during the COVID-19 lockdown, the air quality in Wuhan significantly improved (the air pollution data of Wuhan city available online: <http://sthjt.hubei.gov.cn/hjsj/>, accessed on 15 August 2022), darkening the sky after midnight.

4.2. Brightening of the Night-Time Sky on 21 February 2020

The urban night-time skyglow at various time intervals in Guangbutun region, Wuhan, China, was reduced following the COVID-19 lockdown, as we had anticipated. This can be explained by the decreasing lighting sources, such as traffic and commercial decorative lights, as well as the advanced shutdown timing of night-time lights after entering the lockdown. However, the night-time sky brightness of Guanbutun region suddenly increased on the night of February 21. For instance, from 21:30 to 22:00, the average ZSB increased from 15.6 mcd/m² to 24.5 mcd/m². This phenomenon could be caused by either a change in air conditions or a sudden increase in NTL.

Concerning the first possibility, we found a trend of increasing atmospheric pollutant levels in Wuhan near 21 February 2020. We collected air quality data in Hongshan District during the lockdown, where the observation site is located, and examined the correlation between the concentrations of various atmospheric pollutants and the ZSB at different time intervals around midnight. Table 5 presents the concentrations of PM2.5 and PM10 particles and the ZSB value at the three time intervals in February 2020, and we performed correlation analysis with the values between 16 and 23 February.

Table 5. Zenith sky brightness (ZSB) at the three time intervals of Guangbutun region versus concentrations of PM2.5 and PM10 particles for February 2020. Due to effects of the moon and the cloud cover, the brightness data were null for some dates.

Date	$\mu\text{g}/\text{m}^3$		ZSB (mcd/m ²)		
	PM 2.5	PM10	22:30–23:00	23:30–24:00	After Midnight
4 February 2020	50	57	/	/	7.00
5 February 2020	81	91	/	/	6.73
16 February 2020	12	20	10.3	8.93	5.63
17 February 2020	12	22	9.35	8.30	5.30
19 February 2020	24	30	11.2	9.50	5.20
20 February 2020	34	47	14.0	/	/
21 February 2020	40	47	19.7	16.1	7.14
23 February 2020	31	64	17.9	15.0	/

We found that the ZSB in the late night and concentrations of air pollutants, such as PM2.5 and PM10, both increased during the period 16–23 February. Among them, the concentration of the PM2.5 particle had a clear positive correlation with the ZSB at the time interval of 22:30–23:00 ($R = 0.89$, $p = 0.017$), indicating that deterioration of air quality during this period brightened the night-time sky. However, variations in air quality cannot adequately explain this phenomenon. We also found a more dramatic rise in atmospheric pollutants at the observation site on the previous 4th and 5th of February. Zheng et al. also

noticed this slight pollution event and attributed it to factors, such as home heating [27]. Although PM_{2.5} and PM₁₀ particle concentrations on 4 and 5 February exceeded those on 21 February, the ZSB after midnight on February 5th was not as high as expected (6.73 mcd/m², compared to 7.14 mcd/m²).

Therefore, the brightening of the night-time sky on 21 February 2020 could also indicate an increase in the city's lighting sources, such as the reopening of commercial decorative lights that had been off at the beginning of the lockdown. The explanation may be that when emergency issues related to the epidemic were largely resolved, the resolution to maintain a normal level of night-time urban illumination appeared on the government's agenda. Jechow et al. noticed that several publications advertised that "the lights will stay on during the epidemic" and suggested that NTL may be a symbol of social function in the public mind [25]. We also noticed some similar media reports [39], which showed the decorative lights of Wuhan to express the determination of the government to overcome the epidemic.

However, we had to point out that atmospheric pollutants may contribute to the night-time sky brightness not only from 16 to 21 February but in all the observation periods in this study. In this work, we mainly concentrated on the night-time skyglow dynamics and only made a brief analysis of the influencing factors, and further in-depth analysis was needed in the future to figure out the specific reasons behind.

4.3. Limitation and Future Work

Although SQM has the advantage of long-term observations, the effects of natural factors, such as clouds and moonlight, should be completely removed from the long-term observations since SQM measurements are very sensitive to these natural factors. The cloud product we used in this study was the QF_Cloud_Mask Science Data Set of NASA's daily Black Marble night-time light product suite (VNP46A1). The filtered sky brightness data are directly impacted by the accuracy of the cloud product, which is essential to the conclusions we draw. Furthermore, the majority of cloud products are unable to match SQM's temporal frequency (two minutes in this study). As a result, the influence of clouds could not be entirely removed in our work. Therefore, we need a measurement that can frequently record the spatial distribution of clouds, and a digital camera equipped with a fisheye lens meets our requirements. We think it may be a better choice to use the SQM device in combination with a calibrated, commercial digital camera equipped with a fisheye lens to monitor the night-time skyglow, as mentioned in the review [26]. The fisheye lens can better observe the spatial information of the urban night sky and has a good record of the cloud distribution pattern of the sky at each moment while the commercial camera itself has good stability and helps recalibration of SQM in long-term observation. We are looking forward to the light pollution monitoring effect after the combination of the two methods and are ready to try it in the later light pollution monitoring in Wuhan, China.

Secondly, the single observation site is the main limitation in our study. Although Guangbutun region can be considered as a representative region of Wuhan city, we have to admit that monitoring the sky glow dynamics only in Guangbutun region made us miss some important information, and it was hard to detect all the details of night-time skyglow during the COVID-19 lockdown at the city scale. In fact, there are already some cities that have established monitoring networks using SQMs [40–42]. Therefore, we plan to gradually extend our light pollution monitoring range in subsequent research to form a cross-calibrated monitoring network and eventually to continuously monitor light pollution dynamics in Wuhan at the city level.

5. Conclusions

In summary, we found a general decline and then a rebound in night-time skyglow at various time intervals in Guangbutun region of Wuhan, China during the COVID-19 lockdown. In addition, the fluctuation of the skyglow at different time intervals also decreased. Based on the extracted shutdown timings of lights (STL), we found that parts

of the NTL were shut down earlier after entering the epidemic, causing a significant drop in brightness during some time periods (such as a decrease ratio of 72.1% in the 21:30–22:00 time interval). In contrast, the time intervals around midnight are least affected by the lockdown, with decrease ratios of 32.6%, 24.3%, and 34.4%. The skyglow entered a recovery period on 21 February 2020, and the time intervals before midnight basically returned to the pre-epidemic level, with recovery ratios of 30.4% and 38.2%. However, the skyglow of the 21:30–22:00 time interval only rebounded to 51% of the pre-epidemic level despite a recovery ratio of 22.6%. This is partly due to the fact that, despite the reopening of some of NTL, the shutdown timings of lights during the recovery period were not consistent with those prior to the epidemic. Our results show several aspects about the variation in night-time skyglow in Wuhan, China, during the COVID-19 epidemic lockdown, providing a microscopic viewpoint on the night-time skyglow dynamics impacted by human activities.

Author Contributions: X.L. obtained and provided the main research data; C.L. and C.Z. conceived, designed and performed the experiments; C.L. and X.L. visualized the results and wrote the paper; and all authors edited the paper. All authors have read and agreed to the published version of the manuscript.

Funding: This work was supported by the National Key R&D Program of China under Grant 2019YFE0126800 and Entrepreneurship Training of National Undergraduate of Wuhan University (GeoAI Special Project) under Grant S202110486218.

Acknowledgments: The authors thank Wuhan University Astronomy Association for their instruction in the imagery of the night-time sky with a digital consumer camera with a fisheye lens. We also appreciate the editors and anonymous reviewers for their insightful criticism, which helped us to improve our manuscript.

Conflicts of Interest: The authors declare no conflict of interest.

References

1. World Health Organization (WHO). Coronavirus. Available online: <https://www.who.int/health-topics/coronavirus> (accessed on 22 June 2022).
2. World Health Organization (WHO). Novel Coronavirus (2019-nCoV), Situation Report—3. Available online: <https://www.who.int/docs/default-source/coronaviruse/situation-reports/20200123-sitrep-3-2019-ncov.pdf> (accessed on 22 June 2022).
3. Kupferschmidt, K.; Cohen, J. Can China's COVID-19 strategy work elsewhere? *Science* **2020**, *367*, 1061–1062. [CrossRef]
4. Tian, S.Z.; Feng, R.Y.; Zhao, J.; Wang, L.Z. An Analysis of the Work Resumption in China under the COVID-19 Epidemic Based on Night Time Lights Data. *ISPRS Int. J. Geo-Inf.* **2021**, *10*, 614. [CrossRef]
5. Jia, J.S.S.; Lu, X.; Yuan, Y.; Xu, G.; Jia, J.M.; Christakis, N.A. Population flow drives spatio-temporal distribution of COVID-19 in China. *Nature* **2020**, *582*, 389–394. [CrossRef] [PubMed]
6. Shen, M.; Peng, Z.; Guo, Y.; Xiao, Y.; Zhang, L. Lockdown may partially halt the spread of 2019 novel coronavirus in Hubei province, China. *MedRxiv* **2020**. [CrossRef]
7. Lau, H.; Khosrawipour, V.; Kocbach, P.; Mikolajczyk, A.; Schubert, J.; Bania, J.; Khosrawipour, T. The positive impact of lockdown in Wuhan on containing the COVID-19 outbreak in China. *J. Travel Med.* **2020**, *27*. [CrossRef] [PubMed]
8. Straka, W.; Kondragunta, S.; Wei, Z.G.; Zhang, H.; Miller, S.D.; Watts, A. Examining the Economic and Environmental Impacts of COVID-19 Using Earth Observation Data. *Remote Sens.* **2021**, *13*, 5. [CrossRef]
9. Levin, N.; Kyba, C.C.M.; Zhang, Q.L.; de Miguel, A.S.; Roman, M.O.; Li, X.; Portnov, B.A.; Molthan, A.L.; Jechow, A.; Miller, S.D.; et al. Remote sensing of night lights: A review and an outlook for the future. *Remote Sens. Environ.* **2020**, *237*, 111443. [CrossRef]
10. Falchi, F.; Cinzano, P.; Duriscoe, D.; Kyba, C.C.M.; Elvidge, C.D.; Baugh, K.; Portnov, B.A.; Rybnikova, N.A.; Furgoni, R. The new world atlas of artificial night sky brightness. *Sci. Adv.* **2016**, *2*, e1600377. [CrossRef] [PubMed]
11. Bara, S.; Rodriguez-Aros, A.; Perez, M.; Tosar, B.; Lima, R.; de Miguel, A.D.; Zamorano, J. Estimating the relative contribution of streetlights, vehicles, and residential lighting to the urban night sky brightness. *Light. Res. Technol.* **2019**, *51*, 1092–1107. [CrossRef]
12. Barentine, J.C.; Kundracik, F.; Kocifaj, M.; Sanders, J.C.; Esquerdo, G.A.; Dalton, A.M.; Foott, B.; Grauer, A.; Tucker, S.; Kyba, C.C.M. Recovering the city street lighting fraction from skyglow measurements in a large-scale municipal dimming experiment. *J. Quant. Spectrosc. Radiat. Transf.* **2020**, *253*, 107120. [CrossRef]
13. Jechow, A. Observing the Impact of WWF Earth Hour on Urban Light Pollution: A Case Study in Berlin 2018 Using Differential Photometry. *Sustainability* **2019**, *11*, 750. [CrossRef]
14. Jechow, A.; Ribas, S.J.; Domingo, R.C.; Holker, F.; Kollath, Z.; Kyba, C.C.M. Tracking the dynamics of skyglow with differential photometry using a digital camera with fisheye lens. *J. Quant. Spectrosc. Radiat. Transf.* **2018**, *209*, 212–223. [CrossRef]

15. Sciezor, T.; Kubala, M. Particulate matter as an amplifier for astronomical light pollution. *Mon. Not. R. Astron. Soc.* **2014**, *444*, 2487–2493. [[CrossRef](#)]
16. Jechow, A.; Kollath, Z.; Ribas, S.J.; Spoelstra, H.; Holker, F.; Kyba, C.C.M. Imaging and mapping the impact of clouds on skyglow with all-sky photometry. *Sci. Rep.* **2017**, *7*, 6741. [[CrossRef](#)] [[PubMed](#)]
17. Jechow, A.; Holker, F.; Kyba, C.C.M. Using all-sky differential photometry to investigate how nocturnal clouds darken the night sky in rural areas. *Sci. Rep.* **2019**, *9*, 1391. [[CrossRef](#)] [[PubMed](#)]
18. Puschnig, J.; Schwoppe, A.; Posch, T.; Schwarz, R. The night sky brightness at Potsdam-Babelsberg including overcast and moonlit conditions. *J. Quant. Spectrosc. Radiat. Transf.* **2014**, *139*, 76–81. [[CrossRef](#)]
19. Jechow, A.; Holker, F. Snowglow—The Amplification of Skyglow by Snow and Clouds Can Exceed Full Moon Illuminance in Suburban Areas. *J. Imaging* **2019**, *5*, 69. [[CrossRef](#)] [[PubMed](#)]
20. Katz, Y.; Levin, N. Quantifying urban light pollution—A comparison between field measurements and EROS-B imagery. *Remote Sens. Environ.* **2016**, *177*, 65–77. [[CrossRef](#)]
21. Bustamante-Calabria, M.; de Miguel, A.S.; Martin-Ruiz, S.; Ortiz, J.L.; Vilchez, J.M.; Pelegrina, A.; Garcia, A.; Zamorano, J.; Bennie, J.; Gaston, K.J. Effects of the COVID-19 Lockdown on Urban Light Emissions: Ground and Satellite Comparison. *Remote Sens.* **2021**, *13*, 258. [[CrossRef](#)]
22. Ges, X.; Bara, S.; Garcia-Gil, M.; Zamorano, J.; Ribas, S.J.; Masana, E. Light pollution offshore: Zenithal sky glow measurements in the mediterranean coastal waters. *J. Quant. Spectrosc. Radiat. Transf.* **2018**, *210*, 91–100. [[CrossRef](#)]
23. Kollath, Z. Measuring and modelling light pollution at the Zselic Starry Sky Park. In Proceedings of the 5th Workshop of Young Researchers in Astronomy and Astrophysics, Eotvos Univ, Budapest, Hungary, 2–4 September 2009.
24. Jechow, A.; Kyba, C.C.M.; Holker, F. Mapping the brightness and color of urban to rural skyglow with all-sky photometry. *J. Quant. Spectrosc. Radiat. Transf.* **2020**, *250*, 106988. [[CrossRef](#)]
25. Jechow, A.; Holker, F. Evidence That Reduced Air and Road Traffic Decreased Artificial Night-Time Skyglow during COVID-19 Lockdown in Berlin, Germany. *Remote Sens.* **2020**, *12*, 3412. [[CrossRef](#)]
26. Hanel, A.; Posch, T.; Ribas, S.J.; Aube, M.; Duriscoe, D.; Jechow, A.; Kollath, Z.; Lolkema, D.E.; Moore, C.; Schmidt, N.; et al. Measuring night sky brightness: Methods and challenges. *J. Quant. Spectrosc. Radiat. Transf.* **2018**, *205*, 278–290. [[CrossRef](#)]
27. Zheng, S.; Fu, Y.Y.; Sun, Y.; Zhang, C.J.; Wang, Y.S.; Lichtfouse, E. High resolution mapping of nighttime light and air pollutants during the COVID-19 lockdown in Wuhan. *Environ. Chem. Lett.* **2021**, *19*, 3477–3485. [[CrossRef](#)] [[PubMed](#)]
28. Shao, Z.F.; Tang, Y.; Huang, X.; Li, D.R. Monitoring Work Resumption of Wuhan in the COVID-19 Epidemic Using Daily Nighttime Light. *Photogramm. Eng. Remote Sens.* **2021**, *87*, 197–206. [[CrossRef](#)]
29. Li, X.; Li, X.Y.; Li, D.R.; He, X.J.; Jendryke, M. A preliminary investigation of Luojia-1 night-time light imagery. *Remote Sens. Lett.* **2019**, *10*, 526–535. [[CrossRef](#)]
30. Jiang, W.; He, G.; Long, T.; Guo, H.; Yin, R.; Leng, W.; Liu, H.; Wang, G. Potentiality of Using Luojia 1-01 Nighttime Light Imagery to Investigate Artificial Light Pollution. *Sensors* **2018**, *18*, 2900. [[CrossRef](#)]
31. Den Outer, P.; Lolkema, D.; Haaima, M.; Van der Hoff, R.; Spoelstra, H.; Schmidt, W. Stability of the Nine Sky Quality Meters in the Dutch Night Sky Brightness Monitoring Network. *Sensors* **2015**, *15*, 9466–9480. [[CrossRef](#)]
32. Schnitt, S.; Ruhtz, T.; Fischer, J.; Hölker, F.; Kyba, C.C.M. Temperature Stability of the Sky Quality Meter. *Sensors* **2013**, *13*, 12166–12174. [[CrossRef](#)] [[PubMed](#)]
33. Kyba, C.C.M.; Ruhtz, T.; Fischer, J.; Holker, F. Cloud Coverage Acts as an Amplifier for Ecological Light Pollution in Urban Ecosystems. *PLoS ONE* **2011**, *6*, e17307. [[CrossRef](#)]
34. Roman, M.O.; Wang, Z.S.; Sun, Q.S.; Kalb, V.; Miller, S.D.; Molthan, A.; Schultz, L.; Bell, J.; Stokes, E.C.; Pandey, B.; et al. NASA’s Black Marble nighttime lights product suite. *Remote Sens. Environ.* **2018**, *210*, 113–143. [[CrossRef](#)]
35. Zhao, X.Z.; Yu, B.L.; Liu, Y.; Yao, S.J.; Lian, T.; Chen, L.J.; Yang, C.S.; Chen, Z.Q.; Wu, J.P. NPP-VIIRS DNB Daily Data in Natural Disaster Assessment: Evidence from Selected Case Studies. *Remote Sens.* **2018**, *10*, 1526. [[CrossRef](#)]
36. Zheng, Y.M.; Shao, G.F.; Tang, L.N.; He, Y.R.; Wang, X.R.; Wang, Y.N.; Wang, H.W. Rapid Assessment of a Typhoon Disaster Based on NPP-VIIRS DNB Daily Data: The Case of an Urban Agglomeration along Western Taiwan Straits, China. *Remote Sens.* **2019**, *11*, 1709. [[CrossRef](#)]
37. Unihedron. SQM-LU-DL Users Manual. Available online: <http://unihedron.com/projects/sqm-lu-dl/> (accessed on 22 June 2022).
38. Garstang, R.H. Model for artificial night-sky illumination. *Publ. Astron. Soc. Pac.* **1986**, *98*, 364–375. [[CrossRef](#)]
39. Beijing Radio & Television Network. Aerial Photograph of Wuhan’s Yangtze River Light Display during the COVID-19 Pandemic. Available online: <https://item.btime.com/44272ipr44f84t8uamu8cj2i8d1> (accessed on 24 July 2022).
40. Pun, C.S.J.; So, C.W. Night-sky brightness monitoring in Hong Kong. *Environ. Monit. Assess.* **2012**, *184*, 2537–2557. [[CrossRef](#)] [[PubMed](#)]
41. Cui, H.; Shen, J.; Huang, Y.; Shen, X.; So, C.W.; Pun, C.S.J. Night sky brightness monitoring network in Wuxi, China. *J. Quant. Spectrosc. Radiat. Transf.* **2021**, *258*, 107219. [[CrossRef](#)] [[PubMed](#)]
42. Pravettoni, M.; Strepparava, D.; Cereghetti, N.; Klett, S.; Andretta, M.; Steiger, M. Indoor calibration of Sky Quality Meters: Linearity, spectral responsivity and uncertainty analysis. *J. Quant. Spectrosc. Radiat. Transf.* **2016**, *181*, 74–86. [[CrossRef](#)]